Low spin structure of the $N=Z$ odd-odd nucleus $^{50}_{25}Mn_{25}$

A. Schmidt,[1] I. Schneider,[1] C. Frießner,[1] A. F. Lisetskiy,[1] N. Pietralla,[1,2] T. Sebe,[3] T. Otsuka,[3] and P. von Brentano[1]
[1]*Institut für Kernphysik, Universität zu Köln, D-50937 Köln, Germany*
[2]*Wright Nuclear Structure Laboratory, Yale University, New Haven, Connecticut 06520-8124*
[3]*Department of Physics, University of Tokyo, Hongo, Bunkyo-ku, Tokyo 113-0033, Japan*
(Received 29 February 2000; published 20 September 2000)

Low spin states in the odd-odd nucleus ^{50}Mn were populated in the ^{50}Cr$(p,n\gamma)^{50}$Mn fusion evaporation reaction at 15 MeV beam energy at the FN-Tandem accelerator in Cologne. γ-angular correlations, $\gamma\gamma$ coincidences, and Compton asymmetries were measured. 21 states of ^{50}Mn were observed, 16 for the first time. Six new spin assignments and two parity assignments were made. Eight multipole-mixing ratios and nine new γ-decay branching ratios were determined for the first time. A full pf-shell model calculation for the low-lying states in ^{50}Mn is compared to the data.

PACS number(s): 21.10.Hw, 21.60.Cs, 23.20.Lv, 27.40.+z

I. INTRODUCTION

Self-conjugate nuclei with nucleon numbers $N=Z$ are the most symmetric systems with respect to the proton neutron degree of freedom. This means that these nuclei are the best objects for testing the isospin symmetry of nuclear forces. Both the $T=1$ and $T=0$ states are available in $N=Z$ nuclei. While two identical nucleons can form only $T=1$ states, proton-neutron pairs can be coupled to $T=0$ as well as to $T=1$ configurations.

The importance of the $T=0$ proton-neutron interaction is evident from the fact that the most simple proton-neutron system, the deuteron, is bound only in the $J^\pi=1^+$, $T=0$ ground state. Other two nucleon systems are unbound. Of course, nuclear states with isospin quantum number $T=0$ can only be found in $N=Z$ nuclei. Due to its unique sensitivity to certain parts of the nucleon-nucleon interaction the structure of $N=Z$ nuclei have become a very active topic of research [1–12]. With the recent developments of large detector arrays as Euroball [13], Gammasphere [14], or very efficient mass separator systems, heavy $N=Z$ nuclei can be studied now up to the doubly closed shell nucleus ^{100}Sn [15].

A particularly interesting problem is the structure of medium mass odd-odd $N=Z$ nuclei, in which the lowest $T=0$ states and $T=1$ states are almost degenerate. In these unique cases one can study the interplay of $T=0$ and $T=1$ structures by means of spectroscopy of bound states. The above mentioned phenomenon is in contrast to other nuclei, including even-even $N=Z$ nuclei where the $(0^+,T=0)$ ground state is separated from excited $T=1$ states by a resonably large energy gap. The occurence of strong magnetic dipole ($M1$) transitions between the lowest $T=0$ and $T=1$ states in odd-odd nuclei along the $N=Z$ line is one more interesting phenomenon [11]. Actually these are the largest known magnetic dipole transitions in atomic nuclei.

An important question is, thus, the identification of $T=0$ states in heavy odd-odd $N=Z$ nuclei and the measurement of their properties. We have investigated the low-spin structure of the odd-odd $N=Z$ nucleus ^{50}Mn up to an excitation energy of $E_x \approx 3.6$ MeV. Thereby, we could considerably enlarge and correct the hitherto known [1,16,17] level scheme of ^{50}Mn.

The experimental setup, methods, and results are described in the next section. In Sec. III the data are discussed in comparison to a calculation done in the framework of the nuclear shell model. A summary is given in Sec. IV.

II. EXPERIMENT AND RESULTS

Low spin states of ^{50}Mn were populated using the fusion evaporation reaction ^{50}Cr$(p,n\gamma)^{50}$Mn at a proton beam energy $E_p=15$ MeV. The beam was delivered by the FN-Tandem accelerator of the University of Cologne. In beam γ-ray spectroscopy was performed with the Osiris-cube spectrometer. The experiment was divided into two parts. In the first part the spectrometer was equipped with six identical Compton-suppressed HPGe detectors at each face of the cube. In the second part a highly efficient composite Cluster detector was mounted vertically above the target thereby replacing one of the forementioned smaller detectors. In both parts of the experiment γ-singles spectra were recorded with an average event rate of 10^4 counts per second per detector. $\gamma\gamma$ coincidences were detected with an average event rate of about 2.5×10^3 events per second. Timing and energies of the $\gamma\gamma$-coincidence events were stored on magnetic tape and were analyzed offline.

A full $\gamma\gamma$-coincidence matrix was sorted in order to establish coincidence relations for the construction of the level scheme of ^{50}Mn. As an example of the data, the γ spectrum observed in coincidence with the decay of the $J_i^\pi=2_1^+$, $T=1$ state to the $J_i^\pi=0_1^+$, $T=1$ ground state is shown in Fig. 1. The full low spin level scheme of ^{50}Mn, which could be determined from our $\gamma\gamma$-coincidence data, is shown in Fig. 2. From the analysis of coincidence spectra, 25 new transitions were placed in the level scheme, establishing 16 new levels. The level scheme given previously in Refs. [1,16,17] could be partly confirmed except for the placements of the 1540, 1573, and 1707 keV γ rays, which were wrongly placed above the 5^+ isomer in the literature [16,17]. The 5^+ isomer at 229 keV excitation energy β^+-decays to ^{50}Cr with a half-life of $t_{1/2}=1.75$ min [16,17]. This level is fed from high spin $T=0$ states [1,18]. We were unable to find linking transitions from our low spin levels to this isomer in the

 ©2000 The American Physical Society

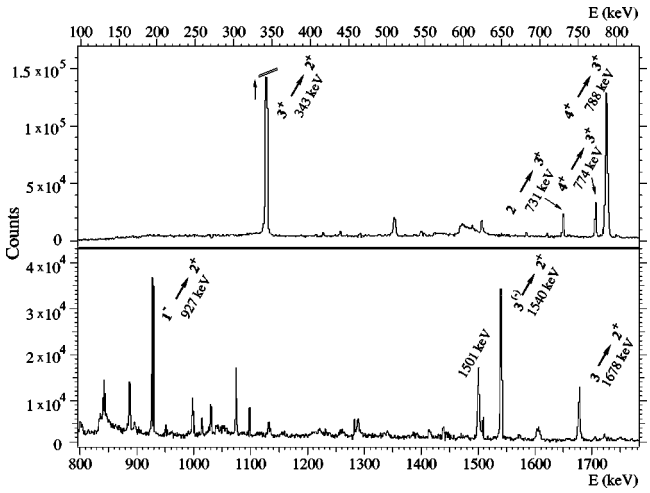

FIG. 1. $\gamma\gamma$-coincidence spectrum observed in the ^{50}Cr$(p,n\gamma)^{50}$Mn fusion-evaporation reaction with a gate on the 800 keV, $2_1^+ \rightarrow 0_1^+$ transition in ^{50}Mn.

(p,n) reaction. Therefore, the isomer shown in Fig. 2 was not established in this work and the excitation energy of 229 keV was taken from other experiments [16,17]. In contrast, we could observe two new levels at 1727 and 1874 keV excitation energy, which decay to the ground state. Table I summarizes our results on excitation energies, transition energies, and decay branching ratios.

For the assignment of spin and parity quantum numbers to excited states of ^{50}Mn it is useful to know the multipole order of γ transitions between them. In order to determine the multipole orders of γ transitions we measured angular correlations of the $\gamma\gamma$ coincidences. Therefore, the coincidence events were sorted offline in a set of coincidence matrices labeled by the geometry of the detectors involved in a given coincidence event. Due to the high symmetry of our cube arrangement many detector pairs contribute to each of the coincidence groups resulting in high statistics of the angular correlation analysis and in reliable spin assignments.

Six new spin quantum numbers were unambiguously established from the analysis of the $\gamma\gamma$ correlations with the methods sketched above and described in more length in Refs. [19,20]. As an example we show in Fig. 3 the $\gamma\gamma$-angular-correlations of the 788–343 keV $4^+ \rightarrow 3_1^+ \rightarrow 2_1^+$ cascade together with the fitted values for two different spin hypotheses for the 4^+ level at 1931 keV. The multipole mixing ratio δ of the $J \rightarrow 3^+$ transition and the Gaussian width σ of the m-substate distribution of the initially oriented level were treated as free parameters. The multipole mixing ratio δ is defined as the ratio of the reduced matrix elements of the transition with multipolarity $\lambda+1$ and the transition with multipolarity λ $(\delta = \langle J_f \| \lambda+1 \| J_i \rangle / \langle J_f \| \lambda \| J_i \rangle)$. It is evident from Fig. 3, that with a spin quantum number hypothesis $J=3$ for the level at 1931 keV the experimental correlation pattern cannot be reproduced by the fit for any quadrupole/dipole mixing ratio of the $J \rightarrow 3^+$ transition. The same holds true for the hypotheses $J=1$ or $J=2$. In contrast, the data are in best accordance with the values for a spin quantum number $J=4$ for the 1931 keV level and a fitted vanishing quadrupole/dipole mixing ratio $\delta = -0.01(2)$. Therefore, we can unambiguously assign the spin quantum number $J=4$ to the level at 1931 keV. In total we could assign six new spin quantum numbers with this method.

To get information about the parity of states, we used in the second part of our experiment the composite Cluster detector as a Compton polarimeter. The sum of two coincident signals, which stem from the Compton scattering of an initial γ quantum in one segment of the Cluster and the subsequent absorption in an adjacent segment, carries the full energy information of the initial γ ray. The geometry of the Compton scattering process depends on the polarization of the initial γ ray with respect to the beam. This enables the measurement of γ polarizations from observable asymmetries of the Compton scattering processes in a Compton polarimeter. For the purpose of parity quantum number assignments it is sufficient to determine the dominant radiation character (E or M) of the corresponding γ transition, if the multipole order and multipole mixing ratios are known already from angular correlations.

The seven large volume Ge crystals of the Cluster detector form a nonorthogonal polarimeter. Numerical simulation [21] as well as recent experiments [12,22] have shown, that the Cluster detector is an efficient Compton polarimeter. The geometry of the Cluster detector implies three polarization groups. We consider adjacent crystal pairs at relative angles

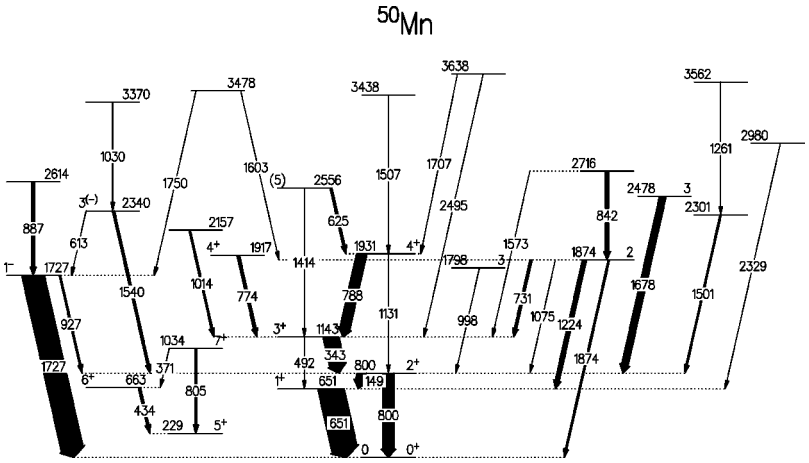

FIG. 2. Low spin level scheme of ^{50}Mn constructed from the $\gamma\gamma$-coincidences obtained in the ^{50}Cr$(p,n\gamma)^{50}$Mn reaction at 15 MeV beam energy. Spin and parity quantum numbers were assigned from the analysis of $\gamma\gamma$-angular correlations and Compton asymmetries. The 5_1^+, 6_1^+, and the 7_1^+ states were taken from Ref. [1].

TABLE I. This table summarizes the information on the low-spin level scheme of ^{50}Mn. We give excitation energies (E_x) of the concluded levels, the γ-transition energies (E_γ), the excitation energies of the final levels (E_f), and the intensity branching ratios I_γ. The levels and transitions which are marked with a star were known from previous experiments [1,16,17]. Those which are marked with a dagger were not observed in our experiment and were added from Ref. [1].

E_x (keV)	E_γ (keV)	E_f (keV)	I_γ (%)
650.8(1)*	650.8(1)*	0.0	100
800.0(1)*	149.2(1)*	650.8	64.1(12)
	800.0(1)*	0.0	100(2)
663†	434†	229†	
1034†	371†	663†	
	805†	229†	
1143.0(1)*	343.0(1)*	800.0	100(2)
	492.0(1)	650.8	1.2(1)
1727.2(2)	927.1(1)	800.0	49.5(12)
	1727.4(2)	0.0	100.0(23)
1797.7(2)	997.7(1)	800.0	100
1874.4(2)*	731.2(2)*	1143.0	34.4(10)
	1074.4(1)	800.0	31(1)
	1223.6(1)*	650.8	100.0(24)
	1874.4(2)	0.0	50.0(15)
1916.6(1)*	773.6(1)*	1143.0	100
1931.0(2)	788.0(1)	1143.0	100(3)
	1131.2(2)	800.0	5.9(8)
2157.3(2)	1014.3(1)	1143.0	100
2300.5(1)	1500.5(1)	800.0	100
2340.2(2)	612.5(2)	1727.2	13.1(14)
	1540.2(2)	800.0	100(3)
2477.7(1)	1677.7(1)	800.0	100
2556.2(1)	625.2(1)	1931.0	100(3)
	1413.9(1)	1143.0	52(2)
2614.4(4)	887.2(4)	1727.2	100
2716.0(1)	841.6(1)	1874.4	100(4)
	1572.8(1)	1143.0	7.6(4)
2980.0(2)	2329.0(2)	651.0	100
3370.2(1)	1030.0(1)	2340.2	100
3438.2(1)	1507.2(1)	1931.0	100
3477.5(3)	1603.0(1)	1874.4	100(6)
	1750.3(1)	1727.2	99(6)
3561.7(2)	1261.2(2)	2300.5	100
3637.5(2)	1706.5(2)	1931.0	29(2)
	2494.9(3)	1143.0	100(6)

of 30°, 90°, and 150° with respect to the reaction plane. The energy of a γ quantum, which is firstly scattered in one crystal and subsequently absorbed in a second adjacent crystal at the relative angle of 30°, 90°, or 150° is sorted in a corresponding pulse height spectrum, at the given sum energy of both coincident events, i.e., at the full energy of the incident γ ray. We denote the different spectra constructed in that way by $N_{30°}$, $N_{90°}$, and $N_{150°}$. The relative intensities of the γ lines in these three different spectra carry the information

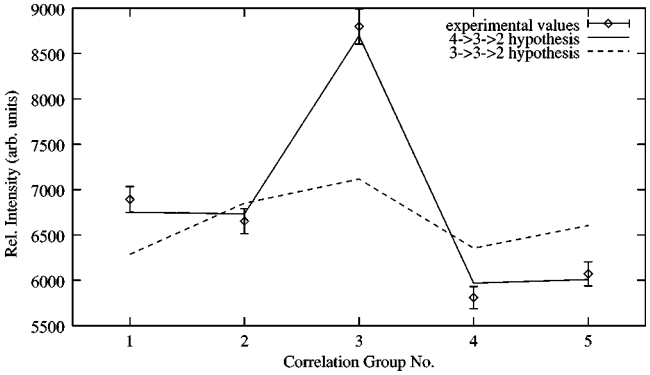

FIG. 3. Experimental and fitted values of the $\gamma\gamma$-angular correlation for the 788–343 keV $4^+ \rightarrow 3_1^+ \rightarrow 2_1^+$ cascade, which connects the levels with an excitation energy of 1931, 1143, and 800 keV, plotted for the different correlation groups of our spectrometer. The quantum numbers for the 3_1^+ state and the 2_1^+ state have been established before from independent data. Only the $J=4$ spin hypothesis for the upper level at 1931 keV can account for the observed correlation pattern. The corresponding multipole-mixing ratio is $\delta=-0.01(2)$. For $J=3$ the hypothesis follows $\delta=-6.1(14)$.

about their radiation character. To extract this information it is convenient to define a polarization asymmetry A:

$$A=\frac{N_{90}-a(N_{30}+N_{150})}{N_{90}+a(N_{30}+N_{150})}.$$

Here the value of the parameter a is determined by the condition that $A=0$ for unpolarized radiation. We obtained $a=0.49$. If we define the beam axis as the x axis, the direction of the Cluster detector as the z axis and correspondingly the

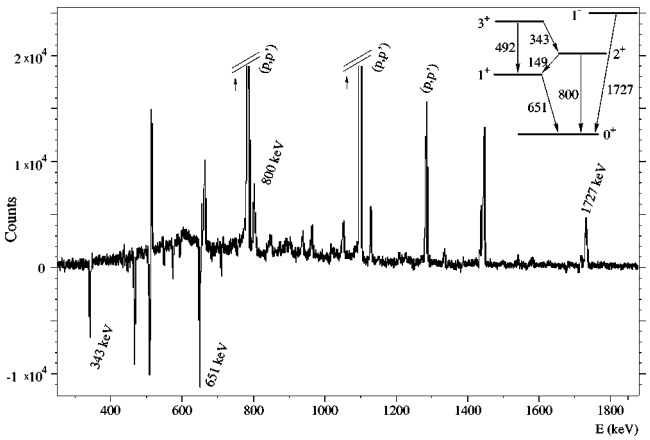

FIG. 4. Part of the difference spectrum N_-. The (p,p')-reaction to ^{50}Cr is the main-reaction channel. The largest γ lines in this spectrum, e.g., at 782 and 1098 keV (the peaks are truncated), stem from known $E2$ transitions in ^{50}Cr. γ transitions of electric character appear as positive peaks and γ transitions of magnetic character appear as negative peaks in the difference spectrum. The 1727 keV $1^\pi \rightarrow 0_1^+$ dipole transition in ^{50}Mn has electric character and, thereby, establishes the parity assignment $\pi=-$ for the 1^- level at 1727 keV.

TABLE II. Summary of experimental information on γ transitions from those excited states of ^{50}Mn, for which spin or parity quantum numbers could be assigned with the $\gamma\gamma$-angular correlation method. The table shows the excitation energy (E), the spin and parity quantum numbers (I^{π}), and the isospin quantum number (T) for the initial and the final levels, the transition energy (E_{γ}), the experimental Compton asymmetry (A), the deduced multipole character ($\mathcal{M}l$), and the quadrupole/dipole mixing ratio (δ). For the 927 keV γ transition, an unambiguous multipole mixing ratio could not be established. Previously known spin and parity values [1,16,17] are marked with a star.

E_i (keV)	E_f (keV)	$I_i^{\pi_i}$ ($\hbar$)	$I_f^{\pi_f}$ ($\hbar$)	T_i	T_f	E_{γ} (keV)	A (%)	$\mathcal{M}l$	δ
651*	0	$1^{+\star}$	0^+	0	1	651	$-2.1(1)$	$M1$	
800*	0	$2^{+\star}$	0^+	1	1	800	4.5(3)	$E2$	
	651		1^+	1	0	149		$M1$	$0.02^{+0.03}_{-0.03}$
1143*	651	$3^{+\star}$	1^+	0	0	492			
	800		2^+	0	1	343	$-4.0(1)$	$M1$	$0.01^{+0.02}_{-0.02}$
1727	0	1^-	0^+	0	1	1727	3.1(1)	$E1$	
	800		2^+	0	1	927			$0.05^{+0.10}_{-0.10}$
									$1.34^{+4.39}_{-0.84}$
1798	800	3	2^+	0	1	998		$E2/M1$	$-0.12^{+0.10}_{-0.10}$
1874*	0	2	0^+	0	1	1874			
	651		1^+	0	0	1223			$-0.01^{+0.02}_{-0.02}$
	800		2^+	0	1	1074			$-3.67^{+0.39}_{-0.49}$
	1143		3^+	0	0	731			$0.00^{+0.03}_{-0.03}$
1917*	1143	$4^{+\star}$	3^+	0	0	774		$E2/M1$	$2.55^{+0.27}_{-0.27}$
1931	800	4^+	2^+	1	1	1131		$E2$	
	1143		3^+	1	0	788		$M1$	$-0.01^{+0.02}_{-0.02}$
2340	800	3	2^+	0	1	1540			$-0.13^{+0.04}_{-0.04}$
	1727		1^-	0	0	613			
2478	800	3	2^+	0	1	1678			$0.01^{+0.06}_{-0.06}$
2556	1143	(5)	3^+	0	0	1414			
	1931		4^+	0	1	625			

direction perpendicular to these two directions as the y axis of the frame of reference, the linear polarization is given by

$$P = \frac{E_x^2 - E_y^2}{E_x^2 + E_y^2},$$

where E_x and E_y are the x and y components of the electrical field vector. One finds the following relation between the experimental asymmetry A and the linear polarization P [23]:

$$A = Q^{\mathrm{pol}}(E_{\gamma}) \cdot P.$$

Here $Q^{\mathrm{pol}}(E_{\gamma})$ is the polarization efficiency of the polarimeter. It is obtained from calibration measurements using radiation with known polarization. We note that $Q^{\mathrm{pol}}(E_{\gamma})$ depends on the energy of the γ-ray E_{γ}. Already the sign of the linear polarization, $\mathrm{sgn}\,P$, is a measure for the electromagnetic radiation character of a transition with pure multipolarity. Since $\mathrm{sgn}\,P = \mathrm{sgn}\,A$, the radiation character of a transition with pure multipolarity can, thus, be determined from the sign of the experimental asymmetry A. If we introduce the difference spectrum $N_- = N_{90} - a(N_{30} + N_{150})$, which is shown in Fig. 4, the γ transitions with positive polarization, which corresponds to the electrical character ($E1$, $E2$, ...) appear as positve peaks, and those with negative polarization, which corresponds to magnetic character ($M1$,$M2$, ...) appear as negative peaks in this spectrum.

The strongest positive peaks in the spectrum N_- come from known $E2$ transitions between levels of ^{50}Cr, excited in the dominant (p,p') reaction channel. The strongest transitions of ^{50}Mn appear as negative peaks, namely the 343 keV $3_1^+ \rightarrow 2_1^+$ transition and the 651 keV $1_1^+ \rightarrow 0_1^+$ transition, demonstrating their dominantly magnetic character. The $2_1^+ \rightarrow 0_1^+ E2$ transition at 800 keV appears as a positive peak showing its electric character. The 1727 keV γ ray appears as a positive peak, too. Together with the spin assignment $J=1$ from the angular correlation analysis only $E1$ character remains possible for the 1727 keV line and we can assign negative parity to the 1^- state at 1727 keV.

The experimental asymmetries we have obtained in this work are given in Table II. In total, we could assign new spin quantum numbers to six levels. Eight new multipole mixing ratios δ were determined. Parity quantum numbers could be established for the two levels at 1727 and 1931 keV from the measured multipole and radiation characters of γ transitions. Table II summarizes the spin and parity quantum number assignments, the multipolarities, the experimental asymmetries, and the multipole mixing ratios δ.

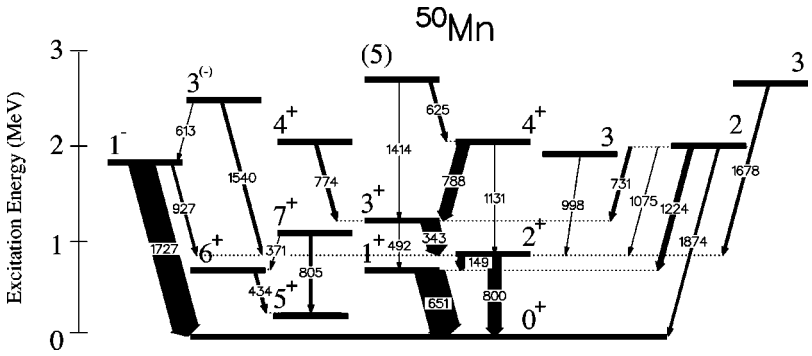

FIG. 5. Part of the ^{50}Mn level scheme, including only those levels for which definite spin or parity quantum numbers are known. The width of the arrows corresponds to the relative intensity of the γ transitions observed in the present reaction. The 5_1^+, 6_1^+, and the 7_1^+ states were added from Ref. [1].

III. DISCUSSION

The new data enlarge considerably our knowledge about the low-lying low spin level scheme of ^{50}Mn. Most valuable for comparison to structure theory are those states for which definite spin assignments are available. To clarify the discussion Fig. 5 shows an excerpt from the level scheme including only those low-spin states with unambiguous spin or parity quantum number assignments. The 0_1^+ ground state, the 2_1^+ state at 800 keV and one of the 4^+ states around 1.92 MeV in ^{50}Mn are interpreted as the $T=1$ isobaric analogs of the 0_1^+ ground state, the 2_1^+ state at 783 keV and the 4_1^+ state at 1882 keV states in the isobaric nucleus ^{50}Cr. Low-lying positive parity states with odd spin quantum numbers and negative parity states must be expected to have the isospin quantum number $T=0$, because such states are missing in ^{50}Cr below an excitation energy of 3 MeV. We found some linking transitions between states with different isospin quantum numbers, e.g., $3_1^+ \rightarrow 2_1^+$, $2_1^+ \rightarrow 1_1^+$, $1_1^+ \rightarrow 0_1^+$, as well as transitions between states with alike isospins, e.g., $3_1^+ \rightarrow 1_1^+$, $2_1^+ \rightarrow 0_1^+$. We could, moreover, extract intensity branching ratios between such isoscalar and isovector transitions, which are summarized in Table I.

The experimental data are compared to shell model (SM) calculations of the positive parity states of ^{50}Mn in the full pf shell without truncation. Two different nucleon-nucleon residual interactions were considered: the KB3 interaction, adopted from Ref. [24] and the FPD6 interaction taken from Ref. [25]. The KB3 interaction is based on the Kuo-Brown G-matrix [26] with modifications of the monopole and some other parts [24], while the matrix elements of the FPD6 interaction are calculated by the OBEP (one boson exchange potential) type functions, whose parameters are chosen so that experimental data of light pf-shell nuclei were reproduced well. The doubly closed-shell nucleus ^{40}Ca is considered as the inert core. The Hamiltonian matrix in the full pf shell was diagonalized without any truncation using the Tokyo shell model code [27]. The calculated excitation energies for the $T=0$ and $T=1$ positive parity levels with spin quantum numbers $J=0-7$ below 4 MeV are compared to the data in Fig. 6. The 5_1^+ isomer and the 6_1^+,7_1^+ states were observed in the high-spin measurement of Ref. [1]. It shows that the calculations lead almost to similar results and to reasonable agreement with experiment.

Both calculations predict the 5^+ isomer to be the first excited state in agreement with the data. The theories consistently predict a peculiarly high-lying 4_1^+ state, around 2 MeV excitation energy. This is actually observed. We note that there is a one-to-one correspondence between the seven observed and calculated positive parity levels below 1.5 MeV.

To obtain a more clear understanding of the experimental results we have calculated $M1$ and $E2$ transition strengths between low-lying states. The results are shown in Table III. Absolute level lifetimes could not be measured directly in the present experiment and, therefore, data on absolute $M1$ and $E2$ transition strengths were indirectly determined only for the $B(E2;2_1^+ \rightarrow 0_1^+)$ and $B(M1;2_1^+ \rightarrow 1_1^+)$ transitions

However, the measured γ-intensity ratios can be compared to the predictions made by the shell model if the calculated transition strengths are used. Table III compares the observed branching ratios and $E2/M1$ multipole mixing ratios δ with those calculated from shell-model $B(M1)$ and $B(E2)$ values. Experimental transition energies were used for the calculation of theoretical branching ratios and multi-

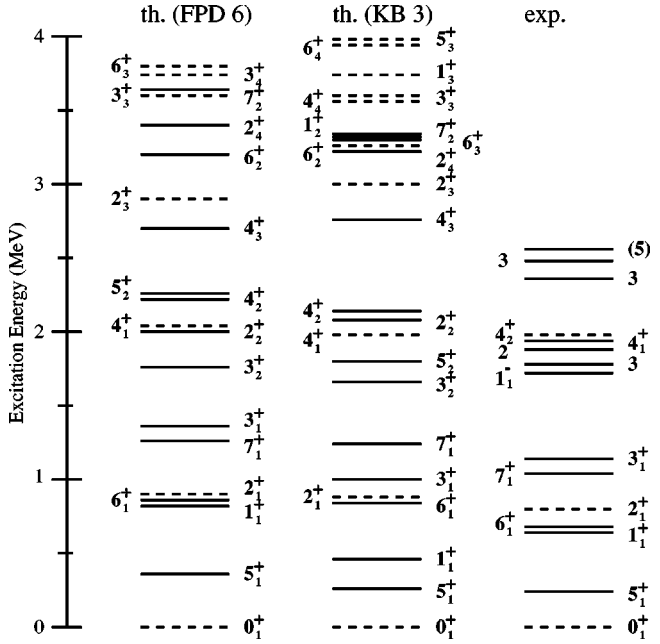

FIG. 6. Comparison of the low-spin level scheme of ^{50}Mn (exp.) to the shell model. Shell model calculations were performed without truncation in the full *pf*-shell with ^{40}Ca as the core. For the residual interaction the KB3 and the FPD6 parametrizations were used. The states with isospin quantum number $T=1$ are plotted with dashed lines and $T=0$ with solid lines. The 5_1^+, 6_1^+, and the 7_1^+ states were added to our results and are taken from Ref. [1].

TABLE III. Comparison of shell model predictions for γ-transition strengths to data on γ-intensity ratios. Calculated $E2$ and $M1$ transition strengths, experimental and calculated branching ratios, and multipole mixing ratios δ in ^{50}Mn are given. Experimental energies were used for the determination of theoretical branching and multipole mixing ratios. Free g factors were used for the KB3 interaction. For the FPD6 interaction we used the effective orbital g factors $g_l^p=0.712$, $g_l^n=0.053$ and the effective spin g factors $g_s^p=6.75$, $g_s^n=-3.41$. The effective proton and neutron charges in the $E2$ operator were chosen to be 1.33 and 0.64, respectively, for FPD6 and 1.5 and 0.5 for the KB3 interaction. The level lifetimes determined from the transition strengths which were calculated with the FPD6 interaction are given in the last column. The data on the $J=2$ state at 1874 keV, the $J=3$ state at 1798 keV, and the $J=(5^+)$ at 2556 keV are labeled with a star and are compared to the calculated values for the $J^\pi=2_2^+$, $J^\pi=3_2^+$, and $J^\pi=5_2^+$ states in the shell model, respectively. The data labeled with a dagger are taken from Svensson *et al.* [1].

$(J_i,T_i)\rightarrow(J_f,T_f)$	$B(E2;J_i\rightarrow J_f)$ (e^2 fm^4)		$B(M1;J_i\rightarrow J_f)$ (μ_N^2)		Branching ratio			δ			τ (ps)
	KB3	FPD6	KB3	FPD6	Expt.	KB3	FPD6	Expt.	KB3	FPD6	FPD6
$(1_1^+,0)\rightarrow(0_1^+,1)$	0	0	2.90	1.49	100	100	100				0.14
$(2_1^+,1)\rightarrow(1_1^+,0)$	0.05	0.02	1.94	1.29	64(1)	128	68	0.02(3)	0.0	0.0	5.4
$(2_1^+,1)\rightarrow(0_1^+,1)$	220	275	0	0	100(2)	100	100				
$(3_1^+,0)\rightarrow(2_1^+,1)$	0.0	0.001	3.73	1.92	100(2)	100	100	0.01(2)	0.0	0.0	0.73
$(3_1^+,0)\rightarrow(1_1^+,0)$	272	350	0	0	1.2(1)	0.4	1.0				
$(3_1^+,0)\rightarrow(5_1^+,0)$	0.28	0.002	0	0		0	0				
$(4^+,1)\rightarrow(3_1^+,0)$	0.2	0.07	2.71	1.99	100(3)	100	100	$-0.01(2)$	0.0	0.0	0.06
$(4^+,1)\rightarrow(2_1^+,1)$	298	385	0	0	5.9(8)	2.9	5.1				
$(4^+,1)\rightarrow(5_1^+,0)$	0.1	0.012	0.04	0.004		15	2.0				
$(5_2^+,0)\rightarrow(4^+,1)$	0.4	1.4	3.46	2.11	100(3)*	100	100				0.09
$(5_2^+,0)\rightarrow(3_1^+,0)$	227	303	0	0	52(2)*	11	23				
$(5_2^+,0)\rightarrow(7_1^+,0)$	55	34	0	0		4	4				
$(5_2^+,0)\rightarrow(6_1^+,0)$	4	2.3	0.4×10^{-5}	7.6×10^{-5}		0.7	0.8				
$(2_2^+,0)\rightarrow(0_1^+,1)$	0.2	0.01	0	0	50(2)*	14	0.4				13
$(2_2^+,0)\rightarrow(1_1^+,0)$	12	4.01	3×10^{-5}	1.6×10^{-3}	100(2)*	100	100	$-0.01(2)$*	6.5	0.51	
$(2_2^+,0)\rightarrow(2_1^+,1)$	0.2	0.021	6×10^{-4}	2.7×10^{-4}	31(1)*	33	9	$-3.67(49)$*	0.2	0.08	
$(2_2^+,0)\rightarrow(3_1^+,0)$	6	2.4	1×10^{-5}	8.1×10^{-4}	34(1)*	4	9.5	0.00(3)*	4.7	0.33	
$(3_2^+,0)\rightarrow(3_1^+,0)$	1.5	2.6	0.2×10^{-5}	1.5×10^{-4}		2	58				1.4
$(3_2^+,0)\rightarrow(2_1^+,1)$	0.001	0.009	6×10^{-4}	1.1×10^{-4}	100(2)*	100	100				
$(3_2^+,0)\rightarrow(1_1^+,0)$	0.9	0.1	0	0		21	13				
$(3_2^+,0)\rightarrow(5_1^+,0)$	40	60	0	0		440	361				
$(4^+,0)\rightarrow(3_1^+,0)$	1.47	0.26	2.2×10^{-5}	2.2×10^{-5}	100	0.3	0.1	2.55(27)	1.7	0.7	2.3
$(4^+,0)\rightarrow(3_2^+,0)$	512	544	1×10^{-5}	0.015		0.0	0.2				
$(4^+,0)\rightarrow(5_1^+,0)$	14	18	4×10^{-6}	5.8×10^{-5}		100	100				
$(4^+,0)\rightarrow(6_1^+,0)$	28	35	0	0		45	52				
$(7_1^+,0)\rightarrow(6_1^+,0)$	285	385	3×10^{-4}	0.01	18(2)†	14	53				28
$(7_1^+,0)\rightarrow(5_1^+,0)$	48	56	0	0	100(2)†	100	100				
$(6_2^+,1)\rightarrow(4^+,1)$	256	340	0	0							
$(6_2^+,1)\rightarrow(5_1^+,0)$	0.1	0.25	0.28	0.26							
$(6_2^+,1)\rightarrow(5_2^+,0)$	0.51	0.13	1.73	0.97							
$(6_2^+,1)\rightarrow(7_1^+,0)$	0.5	0.46	1.52	0.02							
$(6_2^+,1)\rightarrow(7_2^+,0)$	0.24	0.08	1.83	0.96							

pole mixing ratios and transition rates. Finally, total level lifetimes are calculated from the theoretical transition rates.

The good agreement between theory and experiment for the branching ratios and the $E2/M1$ multipole mixing ratios shows that the relative strengths of $M1$ and $E2$ transitions are well accounted for in the shell model. The calculations show the existence of strong $\Delta T=1M1$ transitions between $J_i^\pi=J_1^++1$ and $J_f^\pi=J_1^+$ states with spin quantum numbers $J=0,1,2,3$ in ^{50}Mn. The calculated isoscalar $\Delta T=0$, $\Delta J=2E2$ transitions between these states are strong and comparable for different spin values J of the $J+2\rightarrow J$ transition. It was noted recently in Ref. [12] that similar regularities exist for the low-lying states in the odd-odd nucleus ^{54}Co having predominantly two nucleon $(\pi f_{7/2}^{-1}\times\nu f_{7/2}^{-1})_{J,T}$ structure. The most distinctive feature of this structure is remarkably strong isovector $M1$ transitions. For example, the strength of $M1$ transition from the $2_1^+,T=1$ state to the $1_1^+,T=0$ state (as it was found from the experimental data) amounts to $\sim4.2\mu_N^2$ that is in a very good agreement with the shell model value of 4.6 μ_N^2 (see for the details Ref.

[12]). The strong enhancement of the $M1$ strengths for the two-nucleon $(\pi f_{7/2}^{-1} \times \nu f_{7/2}^{-1})_{J,T}$ configuration is not a unique property of the $f_{7/2}$ orbital. As was recently shown [11] it is a more general property of any one-proton-one-neutron $(\pi j^1 \times \nu j^1)_{J,T}$ configuration with $j=l+1/2$ (e.g., $p_{3/2}$, $d_{5/2}$, $f_{7/2}$, $g_{9/2}$, . . . , orbitals) which is caused by constructive interference of spin and orbital parts of $M1$ matrix elements. Such two-nucleon $(\pi j^1 \times \nu j^1)_{J,T}$ partitions coupled to the even-even $J^\pi=0^+$, $T=0$ core where called *quasideuteron* configurations [11].

Turning back to the ^{50}Mn nucleus, we note that calculated $M1$ strengths for the yrast states in ^{50}Mn are reduced by more than factor two comparing to the similar transitions in ^{54}Co. We expect that this reduction could be understood as due to the coupling of the quasideuteron $(\pi f_{7/2}^1 \times \nu f_{7/2}^1)_{J,T}$ configuration to the $J^\pi \geqslant 0^+$ states of the rotational even-even ^{48}Cr core nucleus. This model requires more detailed formulation and description that is unfortunately beyond the goals of the present paper.

Having the indication of very strong $M1$ transitions one should note that the strong $(3_1^+,T=0) \rightarrow (1_1^+,T=0)$ and $(4^+,T=1) \rightarrow (2_1^+,T=1)E2$ transitions in ^{50}Mn mentioned above carry only a small part of the total decay intensities of the $(3_1^+,T=0)$ and $(4^+,T=1)$ states. The main decay intensity is due to the isovector $M1$ transitions to the yrast states with spin quantum numbers $J-1$. The shell model result is in agreement with experiment. Also the $(2_1^+,T=1)$ state decays by an isovector $M1$ transition to the 1_1^+ state. However, because of the small $2_1^+ \rightarrow 1_1^+$ transition energy the intensity of the $(2_1^+,T=1) \rightarrow (0_1^+,T=1)$ isoscalar $E2$ transition is larger than the intensity of the $(2_1^+,T=1) \rightarrow (1_1^+,T=0)M1$ transition. This observation agrees with the calculation using the FPD6 interaction while the KB3 interaction results in a slightly larger intensity of the $(2_1^+,T=1) \rightarrow (1_1^+,T=0)M1$ transition, probably due to the use of free g factors in KB3.

Furthermore, it is interesting to note that the calculated isovector $M1$ transition between the $(4^+,T=1)$ and $(5_1^+,T=0)$ states and the isoscalar $E2$ transition between the $(3_1^+,T=0)$ and $(5_1^+,T=0)$ states are very weak and not observed in experiment, too. These transitions fall out from the systematics on quasideuteron configurations discussed above since they do not exhibit the expected enhancement. It may be that the $(5_1^+,T=0)$ state has a structure different from the structure of the $0_1^+,1_1^+,2_1^+,3_1^+$ and $(4^+,T=1)$ states. The $(5_1^+,T=0)$ state is connected, however, with the $(7_1^+,T=0)$ and $(6_1^+,T=0)$ states by $E2$ transitions. These transitions were actually observed in experiment [1] but not in the present low-spin study. Neither in our experiment nor in the previous high-spin work [1] was it possible to identify linking transitions between the structure of low-lying low-spin states with isospin quantum numbers $T=0$ or $T=1$ to the $(5_1^+,T=0)$, $(7_1^+,T=0)$, and $(6_1^+,T=0)$ states. Therefore, our results support the hypothesis [1] of a $T=0$ band built on top of the low-lying $(5_1^+,T=0)$ isomer, and indicate that the $(7_1^+,T=0)$ state belongs to this band.

Instead of the 5_1^+ state the calculated $(5_2^+,T=0)$ state is characterized by a strong $M1$ transition to $(4^+,T=1)$ state and a strong $E2$ transition to the $(3_1^+,T=0)$ state, that are in agreement with the observed regularities for the $0_1^+,1_1^+,2_1^+,3_1^+$ and $(4^+,T=1)$ states. The calculated branching ratios for 5_2^+ state are close to the experimental ones for the (5^+) level observed at 2556 keV. Also the excitation energy calculated for the $(5_2^+,T=0)$ state does not differ much from the observations, which indicate that the (5^+) level may have the same quasideuteron structure as the 0_1^+, 1_1^+, 2_1^+, 3_1^+, and 4^+, $T=1$ states. The shell model predicts also a significantly stronger $(6_2^+,T=1) \rightarrow (5_2^+,T=0)\,M1$ transition as the $(6_2^+,T=1) \rightarrow (5_1^+,T=0)$, that gives additional theoretical support to this hypothesis about the (5^+) level at 2556 keV.

The experimental branching ratios which involve isoscalar $(T=1) \rightarrow (T=1)$ and isovector $\Delta T=1$ transitions are very interesting because of one more reason: They can provide an estimate [12] of isovector γ-transition strengths between bound $T=0$ and $T=1$ states, which can be seen practically only in odd-odd $N=Z$ nuclei. Such an estimate can be achieved by assuming a correspondence of the $(T=1) \rightarrow (T=1)$ transition strengths in the odd-odd $N=Z$ nucleus with the strengths of the appropriate isoscalar transitions in neighboring $N=Z+2$ even-even $T_z=1$ isobars, which are often much easier to measure or known already in the literature. One example for such an isoscalar/isovector branching ratio in ^{50}Mn is given by the decays of the $(2_1^+,T=1)$ state to the lower lying $(1_1^+,T=0)$ state and to the 0^+ ground state with $T=1$. In the $T_z=1$ isobaric partner nucleus ^{50}Cr the $2_1^+ \rightarrow 0_1^+$ $(T=1) \rightarrow (T=1)E2$ transition strength is known from Coulomb excitation experiments [28]. If we assume now, that the $(T=1) \rightarrow (T=1)$ $B(E2)$ values are equal for ^{50}Cr and ^{50}Mn, i.e., assuming $B(E2;2_1^+ \rightarrow 0_1^+)_{^{50}\mathrm{Mn}} = B(E2;2_1^+ \rightarrow 0_1^+)_{^{50}\mathrm{Cr}}$, we can estimate the $B(M1)$ value of the isovector $M1$ transition, which connects the 2_1^+ state with the 1_1^+ state. From the measured decay intensity ratio

$$\frac{I_\gamma(2_1^+ \rightarrow 1_1^+)}{I_\gamma(2_1^+ \rightarrow 0_1^+)} = \frac{(1+\delta^2_{2_1^+ \rightarrow 1_1^+})(E_{2_1^+ \rightarrow 1_1^+}/\mathrm{MeV})^3 B(M1)\downarrow/\mu_N^2}{0.70(E_{2_1^+ \rightarrow 0_1^+}/\mathrm{MeV})^5 B(E2)\downarrow/e^2\mathrm{b}^2} = 0.64(1) \quad (1)$$

in ^{50}Mn and from the $B(E2;2_1^+ \rightarrow 0_1^+)=19.8(11)$W.u. $[0.0217(12)\ e^2\,\mathrm{b}^2]$ in the $T=1$ isospin partner nucleus ^{50}Cr [28], we determine in this way

$$B(M1;2_1^+,T=1 \rightarrow 1^+,T=0)_{\mathrm{est}} = 0.97\mu_N^2. \quad (2)$$

This estimated $M1$ transition strength is remarkably large. It is just slightly smaller than the corresponding $B(M1)$ values from the full *pf*-shell model calculations using the FPD6 interaction (see Table III).

Furthermore, we would like to comment on the ''doublet'' of 4^+ states around 1.92 MeV. The spin and parity quantum number assignment $J^\pi=4^+$ for the level at 1931 keV was unambiguously determined from our experiment as it was discussed above (see Fig. 3). The quantum number

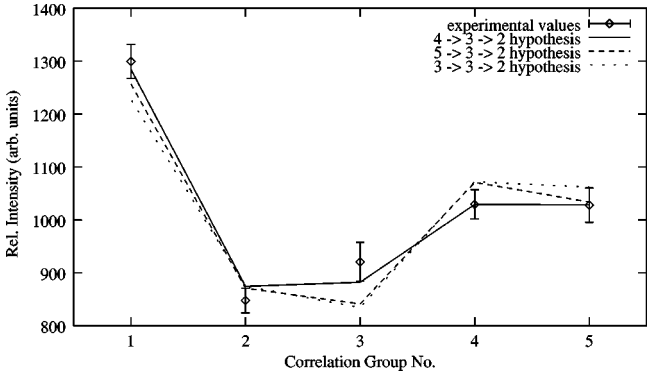

FIG. 7. Angular correlation pattern of the 774–343 keV cascade which connects the levels at 1917, 1143, and 800 keV. Analogous to Fig. 3. We cannot determine unambiguously the spin and parity quantum numbers for the level at 1917 keV from our data. The spin assignment $J=4$ ($\chi^2=0.9$) is most likely. However, alternative spin hypotheses $J=3$ or $J=5$ cannot be fully excluded because of their relatively small $\chi^2\approx 4$ values. Therefore the spin assignment $J^\pi=4^+$ for the level at 1917 keV is taken from Ref. [1].

assignment $J^\pi=4^+$ for the level at 1917 keV could, however, not be uniquely determined from our data. Figure 7 shows the angular correlation pattern that we observed for the $(4^+)\rightarrow 3_1^+\rightarrow 2_1^+$ $\gamma\gamma$ cascade. It is inconclusive. Although the hypothesis $J=4$ matches the data best and is more likely because it shows the smaller χ^2-value of the fit, we cannot completely rule out the alternative spin quantum numbers $J=3$ or 5. For the following discussion we adopt, therefore, the spin quantum number assignment $J^\pi=4^+$ for the level at 1917 keV from the earlier work by Svensson *et al.* [1], which aimed at the investigation of high spin states of ^{50}Mn. From comparison to the isospin multiplet partner nucleus ^{50}Cr we know that one of these 4^+ states must have an isospin quantum number $T=1$ while the other has $T=0$. Under the assumption that the 1917 keV state has indeed $J^\pi=4^+$ one has observed a nearly degenerate $T=0$, $T=1$ bound state doublet in ^{50}Mn. These levels are separated by only 14.4(3) keV. Due to their near degeneracy the excitation energies cannot be used to decide which of the two states is the $(4^+,T=0)$ state. However, the decay pattern provides additional information, which can be used to assign isospin quantum numbers. The 4^+ state at 1931 keV decays with a pure $M1$ transition to the 3_1^+ state with $T=0$ and with a much less intense $E2$ transition to the $(2_1^+,T=1)$ state. From the 4^+ state at 1917 keV we could observe only one decay transition to the $(3_1^+,T=0)$ state, which is of mixed quadrupole/dipole multipolarity with dominant $E2$ character. From the dominantly isovector character of the $M1$ transition operator one expects that $(T=0)\rightarrow(T=0)M1$ transitions are suppressed while $(T=1)\rightarrow(T=0)M1$ transitions can even be enhanced. The opposite is true for $E2$ transitions due to the dominantly isoscalar nature of the $E2$ transition operator. Therefore, one must expect that the transition strengths ratios $B(M1;4^+,T=1\rightarrow 3^+,T=0)/B(M1;4^+,T=0\rightarrow 3^+,T=0)$ and $B(E2;4^+,T=0\rightarrow 3^+,T=0)/B(E2;4^+,T=1\rightarrow 3^+,T=0)$ should both be larger than one. In particular, their product

$$P_{4^+}\equiv\frac{B(E2;4^+,T=0\rightarrow 3^+,T=0)}{B(E2;4^+,T=1\rightarrow 3^+,T=0)}\times\frac{B(M1;4^+,T=1\rightarrow 3^+,T=0)}{B(M1;4^+,T=0\rightarrow 3^+,T=0)}\gg 1 \qquad (3)$$

should be much larger than one. The product P_{4^+} can be expressed by the measured $E2/M1$ multipole mixing ratios $\delta_{4^+\rightarrow 3_1^+}$ and the corresponding transition energies depending on the isospin quantum number assignments to the 4^+ states in question. For the choice, that the 4^+ state at 1917 keV has $T=0$ and the 4^+ state at 1931 keV has $T=1$, we obtain

$$P_{4^+}=\frac{\delta^2_{1917\rightarrow 3_1^+}}{\delta^2_{1931\rightarrow 3_1^+}}\left(\frac{788\ \text{keV}}{774\ \text{keV}}\right)^2>5970.$$

For the opposite choice one obtains the inverse result

$$P_{4^+}<\frac{1}{5970}$$

in contradiction to Eq. (3). We, hence, assign the isospin quantum number $T=0$ to the 4^+ state at 1917 keV and $T=1$ to the 4^+ state at 1931 keV.

The $E2/M1$ multipole mixing ratio from the shell model calculation for the decay of the lowest $(4^+,T=0)$ state is comparable to the mixing ratio measured for the $4^+\rightarrow 3_1^+$ transition of the state at 1917 keV (see Table III). This agreement supports the isospin assignments done above. It must be noted, however, that the shell model predicts the $(4^+,T=0)\rightarrow(5_1^+,T=0)$ transition to be much more intense than the $(4^+,T=0)\rightarrow(3_1^+,T=0)$ transition. But the $(4^+,T=0)\rightarrow(5_1^+,T=0)$ transition is not observed at all in the present experiment as well as in the experiment by Svensson *et al.* [1].

Finally, we would like to note that the calculated decay properties of the shell model $(2_2^+,T=0)$ state in ^{50}Mn differ significantly from the experimental decay properties of the $J=2$ level observed at 1874 keV energy. While the experimental branching ratios are in reasonable agreement with the shell model, the multipole mixing ratios are not. The decay scheme of this $J=2$ level resembles the one of the negative parity $J^\pi=2^-$ level at 1366 keV in the odd-odd $N=Z$ nucleus ^{46}V, the low-spin level scheme of which was studied recently [10]. ^{46}V is the particle-hole symmetry partner nucleus of ^{50}Mn in the single-$f_{7/2}$-shell scheme. Therefore, one can expect certain similarities in the level schemes of ^{46}V and ^{50}Mn. The $J=2$ level at 1874 keV in ^{50}Mn could be a candidate for such a low-lying $J^\pi=2^-$ state. However, the measured dominant quadrupole character of the $2\rightarrow 2_1^+$ transition might be hardly explainable under that assumption. Moreover, two out of three $J=3$ levels at 1798, 2340, and 2478 keV could be candidates for negative parity states because there exists only one positive parity $J=3$ state in the shell model calculations in the excitation energy interval between 1.5 and 3.5 MeV. Further experiments, which can de-

cide these questions, and absolute lifetime information are needed to enable a more rigorous test of the shell model predictions for the level scheme and transition strengths.

IV. SUMMARY

In summary we studied low spin states of the odd-odd $N=Z$ nucleus ^{50}Mn with the ^{50}Cr$(p,n\gamma)^{50}$Mn reaction. The low-spin level scheme was extended by 16 new levels to 21 states and by 25 new γ transitions to 32 γ transitions. From $\gamma\gamma$-angular correlation measurements six new unambiguous spins and eight multipole mixing ratios were assigned. Analyzing the polarization data, we were able to assign positive parity to five states and negative parity to one state. Shell model calculations performed in the full pf shell without any truncation reproduce the low-lying positive parity levels, their branching ratios, and multipole mixing ratios quite well. The experimental branching ratios and the shell model indicate the existence of strong isovector $M1$ transitions in ^{50}Mn.

ACKNOWLEDGMENTS

The authors want to thank in particular A. Fitzler, S. Kasemann, and H. Tiesler for help in data taking. We also thank Dr. A. Dewald, Dr. J. Eberth, Professor A. Gelberg, Professor R. V. Jolos, Dr. S. Lenzi, Dr. T. Mizusaki, D. Weißhaar, and Dr. K. O. Zell for helpful discussions. This work was supported in part by the DFG under Contract Nos. Br 799/10-1, Br 799/9-1, Pi 393/1-1 and in part by the Grant-in-Aid for Scientific Research (A)(2)(10304019) from the Ministry of Education, Science and Culture (of Japan) and by the JSPS-DFG Collaboration.

[1] C.E. Svensson, S.M. Lenzi, D.R. Napoli, A. Poves, C.A. Ur, D. Bazzacco, F. Brandolini, J.A. Cameron, G. de Angelis, A. Gadea, D.S. Haslip, S. Lunardi, E.E. Maqueda, G. Martínez-Pinedo, M.A. Nagarajan, C. Rossi Alvarez, A. Vitturi, and J.C. Waddington, Phys. Rev. C **58**, R2621 (1998).

[2] W. Satula and R. Wyss, Phys. Lett. B **393**, 1 (1997).

[3] D. Bucurescu, C. Rossi Alvarez, C.A. Ur, N. Mărginean, P. Spolaore, D. Bazzacco, S. Lunardi, D.R. Napoli, M. Ionescu-Bujor, A. Iordăchescu, C.M. Petrache, G. de Angelis, A. Gadea, D. Foltescu, F. Brandolini, G. Falconi, E. Farnea, S.M. Lenzi, N.H. Medina, Z. Podolyak, M. De Poli, M.N. Rao, and R. Venturelli, Phys. Rev. C **56**, 2497 (1997).

[4] S. Skoda, B. Fiedler, F. Becker, J. Eberth, S. Freund, T. Steinhardt, O. Stuch, O. Thelen, H.G. Thomas, L. Käubler, J. Reif, H. Schnare, R. Schwengner, T. Servene, G. Winter, V. Fischer, A. Jungclaus, D. Kast, K.P. Lieb, C. Teich, C. Ender, T. Härtlein, F. Kock, D. Schwalm, and P. Baumann, Phys. Rev. C **58**, R5 (1998).

[5] G. de Angelis, C. Fahlander, A. Gadea, E. Farnea, W. Gelletly, A. Aprahamian, A. Axelsson, D. Bazzacco, F. Becker, P.G. Bizzeti, A. Bizzeti-Sona, F. Brandolini, D. de Acuña, M. De Poli, J. Eberth, D. Foltescu, S. Lenzi, S. Lunardi, T. Martinez, D.R. Napoli, P. Pavan, C.M. Petrache, C. Rossi Alvarez, D. Rudolph, B. Rubio, S. Skoda, P. Spolaore, G. Thomas, C. Ur, M. Weiszflog, and R. Wyss, Nucl. Phys. **A630**, 426 (1998).

[6] T. Otsuka, Michio Honma, and Takahiro Mizusaki, Phys. Rev. Lett. **81**, 1588 (1998).

[7] D. Rudolph, C.J. Gross, J.A. Sheikh, D.D. Warner, I.G. Bearden, R.A. Cunningham, D. Foltescu, W. Gelletly, F. Hannachi, A. Harder, T.D. Johnson, A. Jungclaus, M.K. Kabadiyski, D. Kast, K.P. Lieb, H.A. Roth, T. Shizuma, J. Simpson, Ö. Skeppstedt, B.J. Varley, and M. Weiszflog, Phys. Rev. Lett. **76**, 376 (1996).

[8] J. Terasaki, R. Wyss, and P.-H. Heenen, Phys. Lett. B **437**, 1 (1998).

[9] S.M. Vincent, P.H. Regan, D.D. Warner, R.A. Bark, D. Blumenthal, M.P. Carpenter, C.N. Davids, W. Gelletly, R.V.F. Janssens, C.D. O'Leary, C.J. Lister, J. Simpson, D. Seweryniak, T. Saitoh, J. Schwartz, S. Törmänen, O. Juillet, F. Nowacki, and P. Van Isacker, Phys. Lett. B **437**, 264 (1998).

[10] C. Frießner, N. Pietralla, A. Schmidt, I. Schneider, Y. Utsuno, T. Otsuka, and P. von Brentano, Phys. Rev. C **60**, 011304 (1999).

[11] A.F. Lisetskiy, R.V. Jolos, N. Pietralla, and P. von Brentano, Phys. Rev. C **60**, 064310 (1999).

[12] I. Schneider, A.F. Lisetskiy, C. Frießner, R.V. Jolos, N. Pietralla, A. Schmidt, D. Weißhaar, and P. von Brentano, Phys. Rev. C **61**, 044312 (2000).

[13] J. Gerl and R.M. Lieder, Euroball III proposal, 1992.

[14] A.O. Macchiavelli, Acta Phys. Hung. New Ser.: Heavy Ion Phys. **6**, 219 (1997).

[15] M. Lewitowicz, R. Anne, G. Auger, D. Bazin, C. Borcea, V. Borrel, J.M. Corre, T. Dörfler, A. Fomichov, R. Grzywacz, D. Guillemaud-Mueller, R. Hue, M. Huyse, Z. Janas, H. Keller, S. Lukyanov, A.C. Mueller, Yu. Penionzhkevich, M. Pfützner, F. Pougheon, K. Rykaczewski, M.G. Saint-Laurent, K. Schmidt, W.D. Schmidt-Ott, O. Sorlin, J. Szerypo, O. Tarasov, J. Wauters, and J. Żylicz, Phys. Lett. B **332**, 20 (1994).

[16] C.M. McKenna, K.W. Kemper, J.D. Fox, J.W. Nelson, and J.B. Ball, Phys. Rev. C **5**, 145 (1972).

[17] W.L. Fadner, J.J. Kraushaar, and L.C. Farwell, Nucl. Phys. **A178**, 385 (1972).

[18] S.M. Lenzi, C.A. Ur, D.R. Napoli, D. Bazzacco, F. Brandolini, J.A. Cameron, G. de Angelis, M. de Poli, E. Farnea, A. Gadea, S. Lunardi, G. Martínez-Pinedo, A. Poves, C. Rossi Alvarez, H. Somacal, and C.E. Svensson, Nuovo Cimento A **111**, 739 (1998).

[19] K.S. Krane, R.M. Steffen, and R.M. Wheeler, Nucl. Data Tables **11**, 351 (1973).

[20] U. Neuneyer, A. Mertens, R. Kühn, I. Wiedenhöver, O. Vogel, M. Wilhelm, M. Luig, K.O. Zell, A. Gelberg, P. von Brentano, and T. Otsuka, Nucl. Phys. **A607**, 299 (1996).

[21] L.M. Garcia-Raffi, J.L. Tain, J. Bea, A. Gadea, L. Palafox, J. Rico, and B. Rubio, Nucl. Instrum. Methods Phys. Res. A **359**, 628 (1995).

[22] R.-D. Herzberg, C. Fransen, P. von Brentano, J. Eberth, J.

Enders, A. Fitzler, L. Käubler, H. Kaiser, P. von Neumann-Cosel, N. Pietralla, V.Yu. Ponomarev, H. Prade, A. Richter, H. Schnare, R. Schwengner, S. Skoda, H.G. Thomas, H. Tiesler, D. Weißhaar, and I. Wiedenhöver, Phys. Rev. C **60**, 051307 (1999).

[23] D. Weißhaar, diploma thesis, University of Cologne, 1996.

[24] A. Poves and A. Zuker, Phys. Rep. **70**, 235 (1981).

[25] W.A. Richter, M.G. van der Merwe, R.E. Julies, and B.A. Brown, Nucl. Phys. **A523**, 325 (1991).

[26] T.T.S. Kuo and G.E. Brown, Nucl. Phys. **A114**, 241 (1968).

[27] T. Sebe (unpublished).

[28] T.W. Burrows, Nucl. Data Sheets **75**, 1 (1995).